



**HAL**  
open science

# One-Pot Microwave-Assisted Synthesis, in Vitro Anti-inflammatory Evaluation and Computer-Aided Molecular Design of Novel Sulfamide-Containing Bisphosphonates Derivatives

A cha Amira, Hacène K'Tir, Zineb Aouf, Taha Khaldi, Houria Bentoumi, Latifa Khattabi, Rachida Zerrouki, Malika Ibrahim-Ouali, Nour-eddine Aouf

## ► To cite this version:

A cha Amira, Hacène K'Tir, Zineb Aouf, Taha Khaldi, Houria Bentoumi, et al.. One-Pot Microwave-Assisted Synthesis, in Vitro Anti-inflammatory Evaluation and Computer-Aided Molecular Design of Novel Sulfamide-Containing Bisphosphonates Derivatives. *ChemistrySelect*, 2022, 7 (28), 10.1002/slct.202201889 . hal-03970751

**HAL Id: hal-03970751**

**<https://amu.hal.science/hal-03970751>**

Submitted on 11 Feb 2023

**HAL** is a multi-disciplinary open access archive for the deposit and dissemination of scientific research documents, whether they are published or not. The documents may come from teaching and research institutions in France or abroad, or from public or private research centers.

L'archive ouverte pluridisciplinaire **HAL**, est destinée au dépôt et à la diffusion de documents scientifiques de niveau recherche, publiés ou non, émanant des établissements d'enseignement et de recherche français ou étrangers, des laboratoires publics ou privés.

## Medicinal Chemistry & Drug Discovery

# One-Pot Microwave-Assisted Synthesis, *In Vitro* Anti-inflammatory Evaluation and Computer-Aided Molecular Design of Novel Sulfamide-Containing Bisphosphonates Derivatives

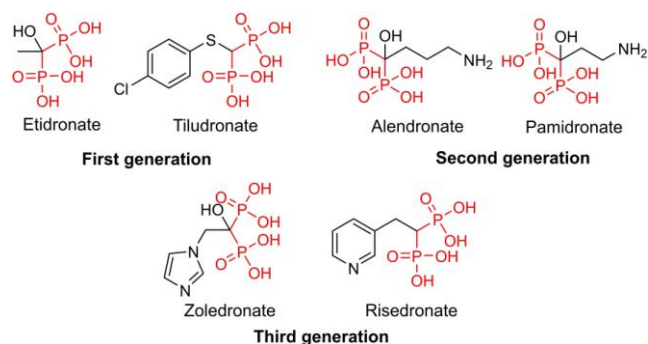
Aïcha Amira,<sup>[a, b]</sup> Hacène K'tir,<sup>[a, c]</sup> Zineb Aouf,<sup>[a]</sup> Taha Khaldi,<sup>[d]</sup> Houria Bentoumi,<sup>[a]</sup> Latifa Khattabi,<sup>[e]</sup> Rachida Zerrouki,<sup>[f]</sup> Malika Ibrahim-Ouali,<sup>[g]</sup> and Nour-Eddine Aouf<sup>[a]</sup>

An eco-friendly and one-step microwave-assisted green synthesis of new functionalized bisphosphonates derivatives was described by a three-component reaction of aromatic sulfamide with triethyl orthoformate and diethyl phosphite. The synthesized compounds were characterized by <sup>1</sup>H, <sup>13</sup>C, <sup>31</sup>P NMR and IR analysis. Some of these compounds were tested for *in vitro* anti-inflammatory activity and showed moderate inhibition compared to diclofenac as standard drug. Furthermore, to rationalize the observed biological data, several *in silico*

approaches have been used to explain Structure-Activity Relationship study (SAR) based on DFT calculation, molecular docking, pharmacodynamic, pharmacokinetic and toxicity profiles of sulfamide-containing bisphosphonates derivatives as anti-inflammatory drugs. The results of the *in vitro* and *in silico* activities prove that the compound **4 b** have the ideal structural requirements for further development of novel anti-inflammatory agents.

## Introduction

More than a decade ago, the synthesis of Etidronate (Scheme 1), a bisphosphonate (BPs) analogue of endogenous pyrophosphate, was described by Menschutkin and later used as an additive to toothpaste and detergent.<sup>[1,2]</sup> In 1970, this



**Scheme 1.** Molecular structure of bisphosphonates derivatives.

bisphosphonate parent compound became the first drug used in the treatment of Paget's disease and osteoporosis.<sup>[3]</sup> Subsequently, other derivatives classified by generation according to their molecular structure appeared (Scheme 1): non-nitrogen bisphosphonates (1<sup>st</sup> generation), alkyl-nitrogen bisphosphonates (2<sup>nd</sup> generation) and heterocyclic nitrogenous bisphosphonates (3<sup>th</sup> generation). These bisphosphonates have different mechanisms of action in their therapeutic efficacy as antiresorptive agents in the treatment of bone disorders,<sup>[4,5]</sup> such as osteoporosis,<sup>[6]</sup> hypocalcaemia,<sup>[7]</sup> multiple myeloma,<sup>[8]</sup> rheumatoid arthritis,<sup>[9]</sup> and bones metastases.<sup>[10]</sup>

Nitrogen bisphosphonates or aminobisphosphonates (N-BPs), the most potent class, strongly inhibit bone resorption, and have a higher binding affinity than non-aminobisphosphonates, due to electrostatic interactions such as hydrogen bonds

[a] Dr. A. Amira, Dr. H. K'tir, Dr. Z. Aouf, Dr. H. Bentoumi, Prof. N.-E. Aouf  
Department of Chemistry  
Applied Organic Chemistry Laboratory, Bioorganic Chemistry Group  
Badji Mokhtar University -Annaba, Box 12,  
Annaba 23000, Algeria

[b] Dr. A. Amira  
National Higher School of Mines and  
Metallurgy-Amar Laskri-Annaba, Algeria  
E-mail: aicha.amira@ensmm-annaba.dz

[c] Dr. H. K'tir  
Medical Sciences Faculty  
Badji-Mokhtar University -Annaba. Box 12,  
Annaba 23000, Algeria

[d] Dr. T. Khaldi  
National Center of Biotechnology Research Constantine (CRBt)  
Ali Mendjli Nouvelle Ville UV 03 BP E73,  
Constantine 25016, Algeria

[e] Dr. L. Khattabi  
Nature and Life Sciences Faculty,  
Brothers Mentouri University, Constantine 1  
BP, 325 Route de Ain El Bey,  
Constantine 25017, Algeria

[f] Prof. R. Zerrouki  
Limoges University, PEIRENE Laboratory, SylvaLim Group  
123 Avenue Albert Thomas Limoges cedex 87060, France

[g] Prof. M. Ibrahim-Ouali  
Aix Marseille University, CNRS  
Centrale Marseille, iSm2, F-13397 Marseille, France

Supporting information for this article is available on the WWW under  
<https://doi.org/10.1002/slct.202201889>

on the hydroxyapatite surface, the main mineral constituent of bone.<sup>[11]</sup>

Furthermore, these compounds have gained considerable attention in the field of medicinal chemistry due to their role in many biological activities, including anti-inflammatory,<sup>[12]</sup> antioxidant,<sup>[13]</sup> antifungal,<sup>[14,15]</sup> antibacterial and antiviral,<sup>[16]</sup> anticancer,<sup>[17]</sup> antiparasitic,<sup>[18]</sup> herbicidal,<sup>[19]</sup> as well as chelating agents.<sup>[20,21]</sup>

However, an additional bioactive functionalized moiety in the bisphosphonate molecule such as 1H-indazole, 1H-pyrazolo[3,4-b]pyridine and 1H-pyrazolo[3,4-b]quinolone,<sup>[22]</sup> 2-amino-benzothiazole,<sup>[23]</sup> nitrogen and sulfur,<sup>[24]</sup> sulfonylamino,<sup>[25]</sup> fluoro-substituted amine,<sup>[26]</sup> pyrazole,<sup>[27]</sup> acrylamide-derived monomer,<sup>[28]</sup> amino acid,<sup>[29]</sup> hyaluronic acid,<sup>[30]</sup> and ethylidene-pyridine bisphosphonate polyoxovanadates complexes,<sup>[31]</sup> give new derivatives for this class of molecules and offer promising and remarkable biological and industrial applications.

In this context, several protocols of the synthesis of nitrogenous bisphosphonates have been developed from carboxylic acids, amides, nitriles, isonitriles, ketophosphonates and the most commonly used procedure is the one-pot three-component condensation of amines with triethyl orthoformate and diethylphosphite.<sup>[32]</sup>

This reaction is carried out in the presence of catalyst such as noble metal nanoparticles AgNps<sup>[33]</sup> and AuNps<sup>[34]</sup>; also, sulfonic acid functionalized hyper-crosslinked polymer HCBP-SO<sub>3</sub>H<sup>[35]</sup> and amberlyst-15<sup>[36]</sup> are used as a heterogeneous catalyst. Moreover, in the presence of CuO<sup>[37]</sup> and rGO-SO<sub>3</sub>H<sup>[24]</sup> under microwave irradiation and solvent-free conditions.

Generally, catalyst-free and solvent-free processes can be achieved using microwave irradiation.<sup>[38,39]</sup>

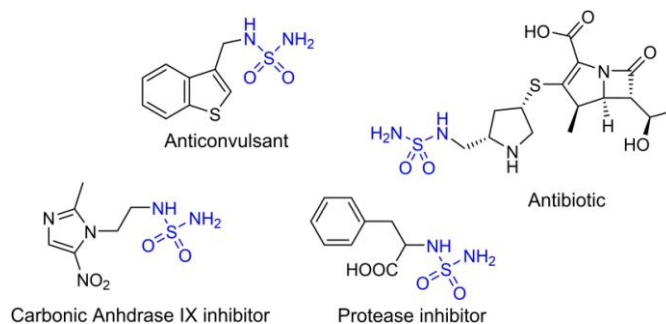
In continuation of our field of study on the synthesis and biological evaluation of organo-phosphorus and -sulfur compounds,<sup>[40-43]</sup> we describe here a simplified three-component one-pot synthesis of sulfamide-containing bisphosphonates derivatives under microwave irradiation. This method respects remarkable principles of green chemistry; atom economy, design for energy efficiency, safety and environment friendly without using any catalyst or solvent, thus reduce chemical waste and reaction time.

Sulfamide is one of the most promising moieties present in many clinically useful drugs and has various biological activities.<sup>[44-48]</sup> (Scheme 2)

Consequently, a simple method for synthesis of new hybrid molecules containing both bisphosphonate and sulfamide motifs would be very useful.

In this work, we report a convenient one-pot reaction of sulfamide-containing bisphosphonates under microwave activation, and four newly synthesized compounds were evaluated for their *in vitro* anti-inflammatory activity. The Structure-Activity Relationship study (SAR) based on DFT calculation were investigated to compare with *in vitro* anti-inflammatory results.

Matrix Metalloproteinases (MMPs), extracellular proteinases family, is one of research therapeutics targets involved in tissue regeneration and thoroughly related to physiologic and physiopathological processes such as inflammation, angio-



**Scheme 2.** Sulfamide derivatives as drugs and medicinal inhibitors.

genesis, and metastasis in cancer.<sup>[49-52]</sup> One of the most potent inhibitors and downregulatory of this target is bisphosphonates derivatives.<sup>[53-55]</sup> In this respect, the molecular docking was realized to determine the most preferred binding mode and hence the mechanism of anti-inflammatory action might be streamlined. To estimate the pharmacokinetic/pharmacodynamics profile in humans of our synthesized compounds, oral bioavailability and absorption, distribution, metabolism and excretion (ADME) descriptors were performed.

## Results and discussion

### Chemistry

Initially, sulfamides **1(a-f)** were prepared from the corresponding amines according to the procedure reported previously by our group.<sup>[56]</sup> Herein, we synthesized a variety of sulfamides from various substituted anilines with electron donating and withdrawing groups.

In the next step, the synthesis of bisphosphonates bearing sulfamide moiety derivatives were started. For this purpose, the reaction of sulfamide **1 a** with triethyl orthoformate **2** and diethyl phosphite **3** under different conditions was examined as summarized in Table 1.

At first, the reaction was conducted under solvent-free conditions at 150 °C for 24 h, the desired product was not formed (Table 1, entry 1). When EtOH was used as a solvent, also no reaction progress was observed (Table 1, entry 2).

On the other hand, using catalysts such as amberlyst-15 (20 mol%) and heteropolyanion (20 mol%) at room temperature did not give the desired result (Table 1, entries 3 and 4).

Alternatively, our efforts have been led to use energy efficient process; we conducted the reaction under ultrasonic irradiation (Table 1, entry 5), only the imine, intermediate product, was formed.

When using microwave activation under solvent-free conditions at different temperatures and powers, bisphosphonate formation was achieved after 10 min at 150 °C and power of 500 W (Table 1, entry 6).

In another experiment, an increase of the diethyl phosphite to 5 equivalents under similar conditions did not improve yield (Table 1, entry 7).



## In vitro anti-inflammatory activity

Protein denaturation is a pathway by which proteins lose their structures as a result of altered hydrogen, hydrophobic, electrostatic, and disulfide bonds. The majority of proteins lose their biological activities as a result of denaturation and cause the generation of autoantigens, leading to a series of autoimmune dysfunctions, such as inflammatory and rheumatoid disorders. Thus, drugs that inhibit protein denaturation are considered essential anti-inflammatory agents.<sup>[57]</sup> Several anti-inflammatory drugs have shown a dose dependent ability to inhibit heat-induced protein denaturation.<sup>[58]</sup>

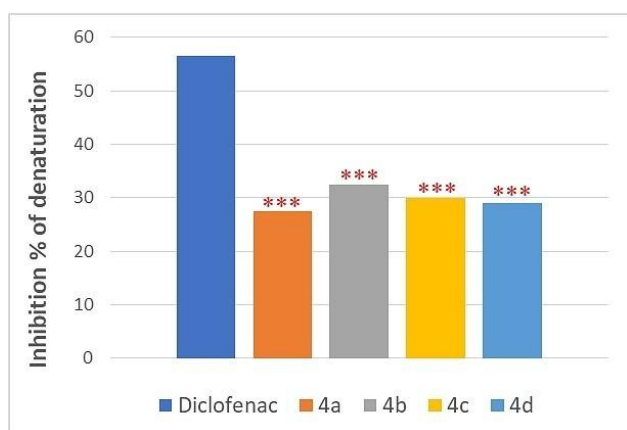


**Figure 1.** *In vitro* anti-inflammatory effect of the studied compounds **4(a-d)**. Data are presented as the mean  $\pm$  standard deviation ( $n=3$ ) \*\*\*  $P < 0.001$  compared to diclofenac group.

The *in vitro* anti-inflammatory effect of sulfamide containing bisphosphonates samples were evaluated by ovalbumin denaturation and the results are shown in Figure 1. The results showed that **4 b** has the ability to stop induced protein denaturation at a dose-dependent proportion, it gives the highest level of inhibition of 32.50 %, followed by **4 c** and **4 d** with a percentage inhibition of 29.95 % and 29.09 % respectively, followed by **4 a** with 27.43 %. A 25 mg/mL dose of diclofenac (0.026 mM) has an anti-inflammatory action with 56.46% of inhibition.

The bulk of our data suggest that the compounds were found to have anti-inflammatory effects and may be a starting point for the development of new compounds to counteract the deleterious effects of inflammatory diseases.

## Theoretical investigation

### Geometry optimization and global reactivity descriptors

The optimized geometries of sulfamide-containing bisphosphonates derivatives **4(a-d)** have been obtained by Gaussian 09 at the B3LYP/6-31G (d,p) level in the gas phase, the optimized structure of the studied compounds are illustrated in Figure 2.

The representation 3D of the frontier molecular orbital LUMO and HOMO calculated in the gas phase for the different bisphosphonates derivatives **4(a-d)** are illustrated in Figure 3.

The energy gaps of compounds **4a**, **4b**, **4c** and **4d** were computed to be 6.03, 5.89, 5.91 and 6.22 eV respectively.

The energy gap in the decreasing order of study compounds is found to be **4d > 4a > 4c > 4b**.

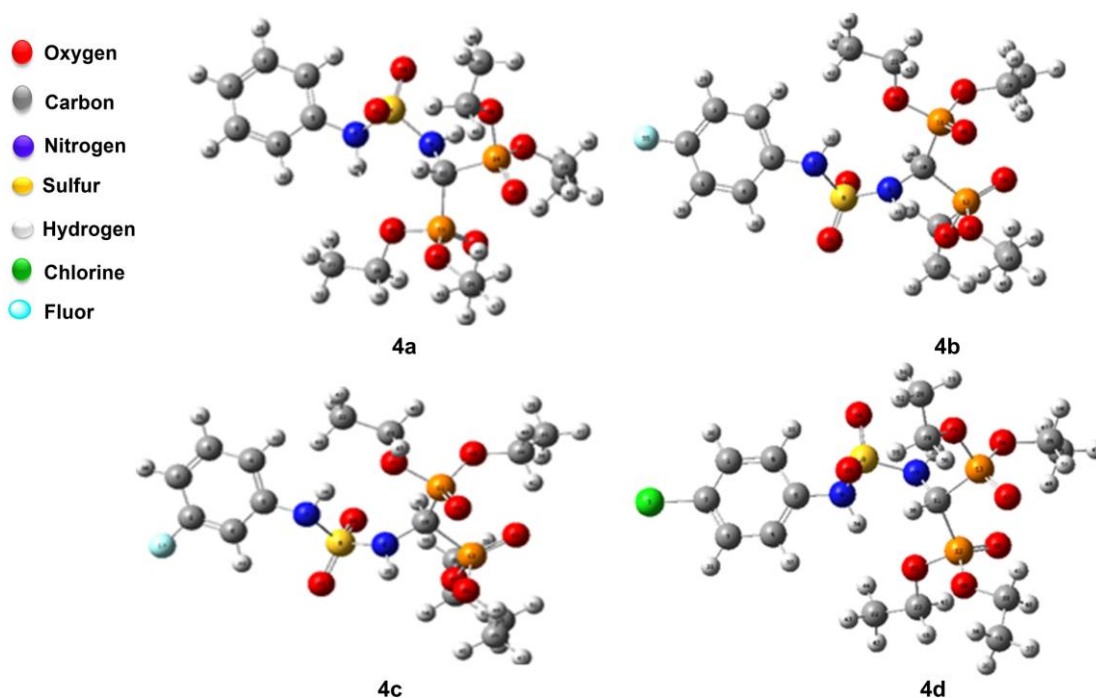


**Figure 2.** The optimized structure of the studied compounds **4(a-d)**.

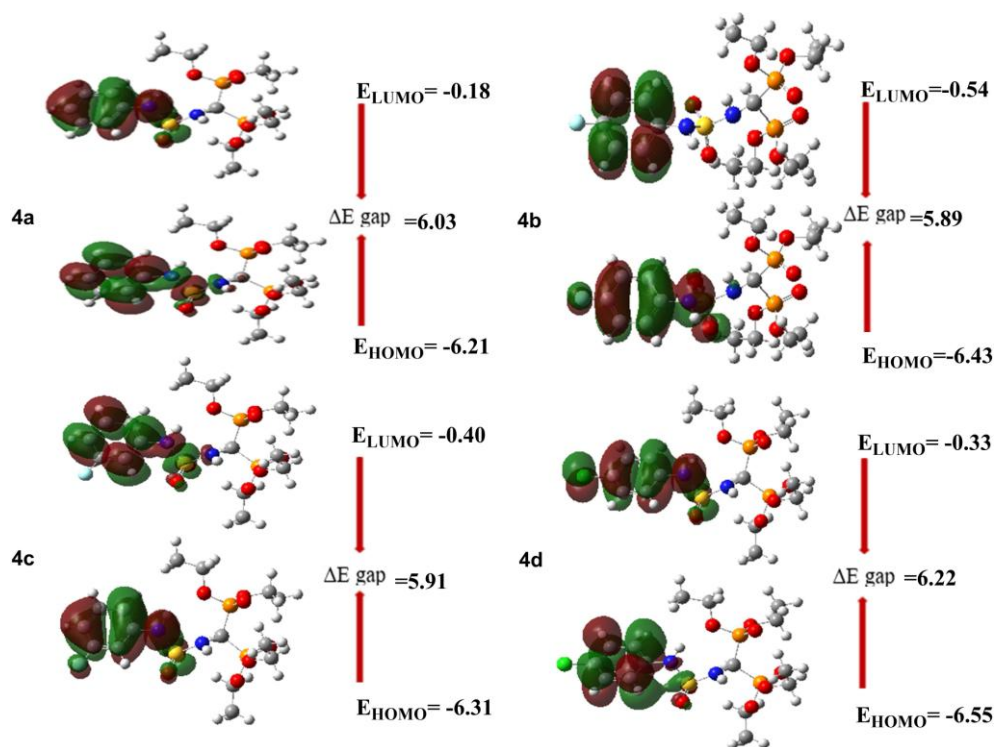


**Figure 3.** 3D representation of HOMO, LUMO and their energy gap ( $\Delta E_{\text{gap}}$ ) of the studied molecules **4(a–d)**.

The electronic properties HOMO-LUMO energies, the total value of the dipole moment, the linear polarizability  $\alpha_{\text{TOT}}$  ( $\text{Bhor}^3$ ) were calculated basing on the optimized structure in the gas phase at the B3LYP/6-31G (d,p) level. The reactivity indices were proposed by Parr and Yang since the 1981, the aim of which is to provide a precise theoretical framework to often ill-defined concepts characterizing chemical reactivity,<sup>[59,60]</sup> such as chemical potential ( $\mu$ ), electronegativity ( $\chi$ ), ionization potential (I), electronic affinity (A), hardness ( $\eta$ ), softness ( $S$ ), electrophilicity ( $\omega$ ) and nucleophilicity ( $N$ ). This model has been judged the most successful and still seems the most promising.<sup>[61]</sup> The results are summarized in Table 2.

The highest value of the energy gap (6.22 eV) and the lowest values of linear polarizability (252.58  $\text{Bhor}^3$ ) investigated is for compound **4d**, while the lowest value of gap (5.89 eV) is for compound **4b** with linear polarizability value (253.57  $\text{Bhor}^3$ ). Therefore, **4b** is less stable and more reactive.

According to the other results, compounds **4b** and **4d** are highly active molecules, because of their higher values of the ionization energy respectively (I= 6.43, 6.55 eV) and small

values of affinity (A = 0.54, 0.33 eV). Therefore, it can be seen that these results are in agreement with anti-inflammatory activity. The highest value of chemical hardness of **4b** (-3.485 eV), describing the molecule as donor electrons.

Based on the classification of organic molecules in the literature, the studied synthesized bisphosphonates **4(a–d)** are classified as strong electrophiles with  $\omega > 1.5$  eV; **4b** and **4d** as moderate nucleophiles with  $2.0 > N > 0$  eV and **4a** and **4c** as strong nucleophiles with  $N > 3.0$ .<sup>[62]</sup>

Additionally, Molecular Electrostatic Potential (MEP) surface analysis, that illustrates the charge distributions of molecules three dimensionally as shown in Figure 4, is used to estimate the chemical reactivity of molecules. In the studied compounds, the positive regions represented by blue color are related to nucleophilic reactivity and showed in the amino groups; the negative regions represented by red and yellow colors are related to electrophilic reactivity and showed in the sulfonyl and phosphite groups.

**Table 2.** Calculated values of the global reactivity descriptors for synthesized bisphosphonates 4(a-d) studied by B3LYP/6-31G (d, p) level in the gas phase.

Gas phase Molecule	E (u.a)	$\mu$ total (D)	$\alpha_{\text{TOT}}$ ( $\text{Bhor}^3$ )	I	A	$\mu$	$\chi$	$\eta$	S	$\Omega$	N
<b>4a</b>	-2380.75	3.38	266.86	6.21	0.18	-3.195	3.195	3.015	0.165	1.692	3.158
<b>4b</b>	-2479.97	3.21	253.57	6.43	0.54	-3.485	3.485	2.945	0.169	2.062	2.938
<b>4c</b>	-2479.98	4.60	253.50	6.31	0.40	-3.355	3.335	2.955	0.169	1.904	3.058
<b>4d</b>	-2495.27	4.23	252.58	6.55	0.33	-3.440	3.440	3.110	0.160	1.902	2.818

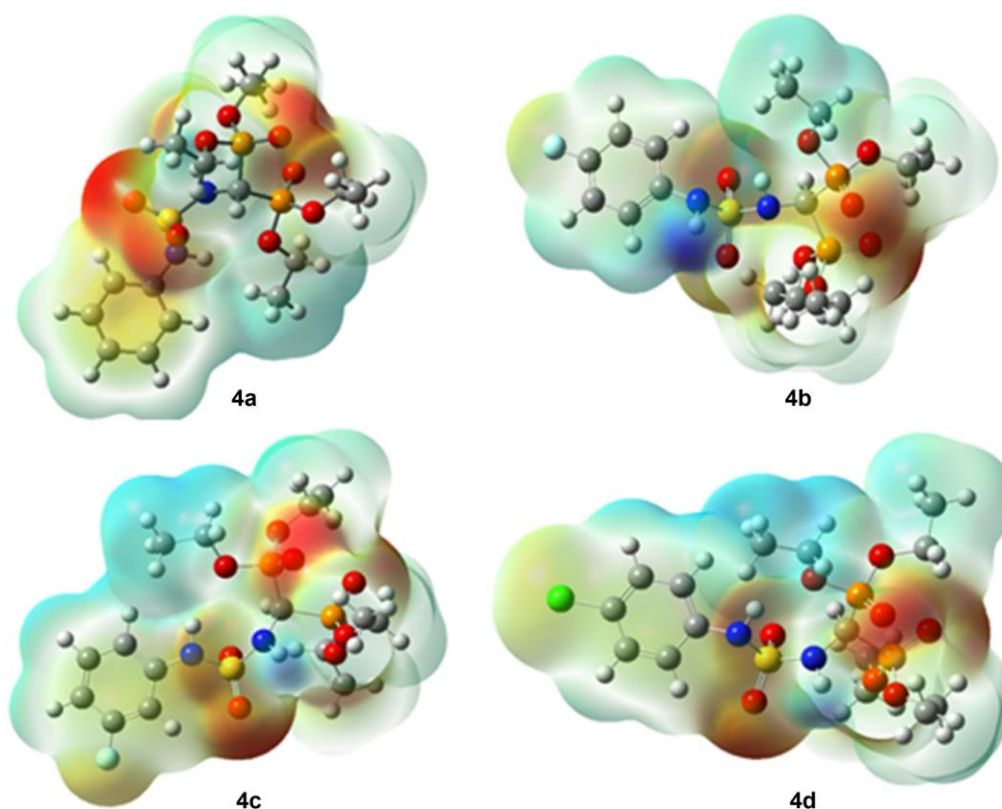


**Figure 4.** MEP formed by mapping of total density over electrostatic potential in gas phase for the synthesized compounds **4(a–d)**.

#### Binding affinities, amino acids interaction of the ligands into MMP-8 active site

The docking results of compounds **4(a–d)** for a potential inhibition of MMP-8 are listed in Table 3.

After checking the results there is a correlation between the *in silico* study with MMP-8 and the experimental activity of the bisphosphonates. Noting the most potent inhibition observed is for **4 b** corresponding to the higher scoring value. For the others dockings, **4 d** showed the less Scoring value, but nevertheless, its inhibition activity is higher comparable to **4 a**. Following that, we considered additional energy interactions

aspects in the docking computation. A schematic illustration of the interactions of the ligands in MMP-8 with bisphosphonates previously synthesized is shown in Figure 5. As indicated in the literature,<sup>[63,64]</sup> bisphosphonates could bind the Zn<sup>2+</sup> ion in a monodentate fashion through the oxygen atom double bonded to the phosphorus atom (P=O) of one of the phosphonates moieties. Only for **4(c–d)**, zinc chelation was observed through the oxygen atom double bonded to the sulfure atom (S=O) of the sulfamide group. In all cases, for the zinc ion, a distorted tetrahedral coordination geometry was detected. It's caused by chelation with residues His 197, His201 and His 207. Moreover, various protein-ligand interactions

**Table 3.** Docking results of compounds **4(a–d)** for a potential inhibition of MMP-8.

	S (Kcal/mol)	Hydrogen bonds	Hydrophobic interactions	Metallic interactions	Ionic interactions	H- $\pi$ interactions	$\pi$ - $\pi$ interactions
A	−10.6548	Gly 155	Arg 222, Tyr 216, Asn 218, Pro 217, Ala 261, Leu 160, Ile 159, Leu 193, Val 194, Leu 214, Glu 198	Zn 304, His197, His201, His207	His201, His207	Tyr 219, Ala 220.	Tyr 219
<b>4a</b>	−9.3675	Ile 159, Leu 160.	Tyr 216, Asn 218, Pro 217, Ala 161, Leu 214, Leu 193, Val 194, Glu 198.	Zn 304, His 197, His 201, His 207.	His 201, His 207.	Tyr 219	His 197
<b>4b</b>	−10.9786	Pro 217, Ile 159, Leu160	Leu 193, Leu 214, Val 194, Tyr 217, Glu 198, Arg 222, Ala 220, Ala 161, Asn 218, Gly 156, His 162	Zn 304, Zn 304, His 197, His 201, His 207.	His 201, His 207.	Tyr 219	His 197
<b>4c</b>	−9.1361	Glu 198, Ala 163	Ile 159, Ser 151, His 162, Phe 164, Val 194, Pro217, Leu 160, Asn 218.	Zn 304, His 197, His 201, His 207.	His 201, His 207.	/	/
<b>4d</b>	−7.3065	Glu 198	Asn 218, Pro 217, Ala 161, Leu 160, Glu 158, His 162, Ile 158.	Zn 304, His 197, His 201, His 207.	His 201, His 207.	Leu 160	/

Foot note: A: co-crystallized Ligand.



shown in Table 4. The co-crystallized ligand has a molecular weight  $\diamond$  500 g/mol, so it doesn't obey Lipinski's first rule. **4(a-d)** and Diclofenac have respectively the following molecular weights: (458.40, 476.39, 476.39, 492.85, 196.15) g/mol, they have all a molecular weight  $\diamond$  500. These molecules have the following Topological Polar Surface Area (TPSA) values (49.33, 157.23, 157.26, 157.26, 157.26) ( $\text{\AA}^2$ ) respectively, the lowest TPSA always give good results. By comparing the lipophilicity (Log P) values of molecules, we find, they all show very good results  $\diamond$  5 and can be easily absorbed in body. However, Diclofenac and molecules **4(a-d)** have NHBA values of (2, 9, 10, 10, 9) and NHBD (2) for all, also molar refractivity (77.55, 107.64, 107.59, 107.59, 112.65). So, we can observe that compounds **4(a-d)** are appropriate by the five Lipinski rules. As conclusion, these results approve those compounds **4(a-d)** can be considered as potential successful drugs.

As shown in Figure 6, the graph of bioavailability radar signifies an initial scan at the drug-likeness of the sulfamide-containing bisphosphonates derivatives synthesized, the pink regions represent the optimum range of the following six

properties: lipophilicity, size, polarity, solubility, saturation and flexibility. The test revealed that all compounds are slightly outside the pink area on side of polarity due to the presence of extra polar atoms, the compounds also show inconformity on the flexibility side. The compounds showed good solubility and saturation properties.

Moreover, the ADMET analysis were predicted and summarized in Table 5. Table S6 In absorption part, Humain intestinal Absorption (HIA) proved that the diclofenac and **4(a-d)** are easily absorbed in intestine. The inhibition of Pgp-glycolprotein ease the transport of many drugs, compared our results of Pgp-glycolprotein, we observed that the **4(a-d)** are easily absorbed in cell. In the distribution part, the Blood-Brain-Barrier BBB protects the brain from exogenous compounds. The BBB permeability is one of the highly important pharmacological parameters which is necessary to help reduce side effects and toxicity or to improve the efficacy of drugs. Based on this analysis, we observed that all compounds (**4 a-d**) give a high capacity to cross into the brain. Furthermore, the result of metabolism part proved that the **4(a-d)** are potential inhibitor

**Table 4.** Druglikeness results of compounds **4(a-d)** for a potential inhibition of MMP-8.

Drug likeness properties	Co-crystallized ligand	Diclofenac	4a	4b	4c	4d
Molecular weight (g/mol)	527.58	196.15	458.40	476.39	476.39	492.85
<b>Consensus Log P (o/w)</b>	−0.42	3.66	1.67	2.07	2.07	2.20
Log S	−1.17	−4.65	−2.46	−2.61	−2.61	−3.04
NHBA	9	2	9	10	10	9
NHBD	5	2	2	2	2	2
Molar refractivity	89.75	77.55	107.64	107.59	107.59	112.65
Bioavailability Score	0.11	0.85	0.55	0.55	0.55	0.55
Synthetic accessibility (SA)	5.44	2.23	4.71	4.71	4.71	4.59
TPSA ( $\text{\AA}^2$ )	189.23	49.33	157.23	157.26	157.26	157.26
N° of rotatable bonds	6	4	14	14	14	14

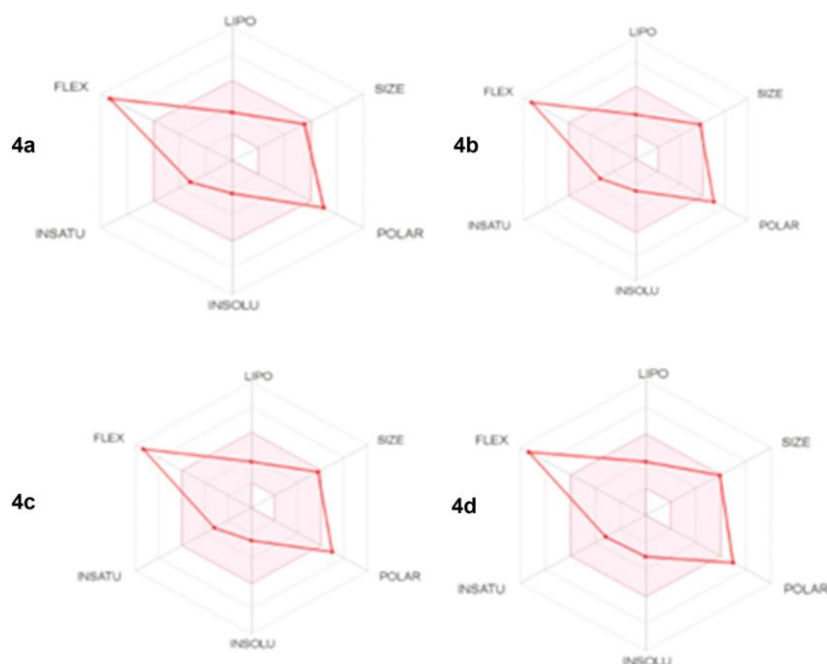


**Figure 6.** Radar related to physicochemical properties of molecules **4(a-d)**.

**Table 5.** The ADME/T test result of ligands (various pharmacokinetic and pharmacodynamic properties).

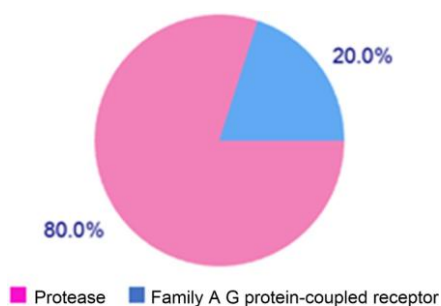
Class	Properties	Co-crystalized ligand	Diclofenac	4a	4b	4c	4d
Absorption	Caco-2 permeability	−0.625	1.379	−0.479	−0.531	−0.38	−0.624
	Pgp-inhibitor	YES	NO	NO	NO	NO	NO
	Pgp-substrate	YES	YES	YES	YES	YES	YES
	Human intestinal Absorption (HIA)	94.964	91.923	81.863	82.373	82.34	82.56
Distribution	BBB (blood-Brain Barrier)	−1.972	0.236	−2.1	−2.253	−2.279	−2.347
Metabolism	CYP1A2 inhibitor	NO	NO	YES	YES	YES	YES
	CYP2C19 inhibitor	YES	NO	YES	YES	YES	YES
	CYP2C9 inhibitor	YES	NO	YES	YES	YES	YES
	CYP2D6 inhibitor	YES	NO	NO	NO	NO	NO
	CYP3A4 inhibitor	NO	NO	NO	NO	NO	NO
Toxicity	hERG (hERG Blockers)	NO	NO	NO	NO	NO	NO
	AMES Toxicity	NO	NO	NO	NO	NO	NO
	Acute oral toxicity	2.212	2.405	2.226	2.026	2.213	3.225

of P450 1 A2, P450 2 C19 and P450 2 C9. In the toxicity part, we confirmed that the compounds **4(a–d)** present negative test. The ADMET analysis proves that the synthesized compounds have acceptable properties as demanded for potential drugs.

In addition, the compounds **4(a–d)** were tested *in-silico* for their molecular target studies. The results of the prediction are shown in Figure 7. The possible target sites may bind to are mostly the protease targets.

## Conclusion

In the present work, a simple and green one-pot protocol was successfully developed for the synthesis of novel sulfamide-containing bisphosphonates derivatives from the reaction of variously substituted aromatic sulfamides, diethyl phosphite, and triethyl orthoformate under microwave irradiation and solvent-free conditions. Four of the title compounds were evaluated for; anti-inflammatory activity by inhibition of protein denaturation method, DFT and ADME/T studies and they were docked against inhibitor MMP-8. The investigation showed remarkable *in vitro* and *in silico* activities, mainly the compound **4b** has the highest anti-inflammatory activity, the lowest gap energy and good affinity to the metal ( $Zn^{2+}$ ) nearest binding site, which can be attributed to the presence of fluoro substituent at the para position. The synthesized target compounds could be used as a lead for new anti-inflammatory agents.

**Figure 7.** Molecular targets prediction for compound **4b**.

## Experimental section

### Chemistry

#### General information

Chemical reagents were purchased from Fluka, Aldrich and Merck companies and were used without further purification. Progress of the reaction was followed by thin layer chromatography (TLC) using silica gel Merck 60 F<sub>254</sub> (Art.5554). Column chromatography was performed using Merck 60 H (Art.9285). IR spectra were determined with a Perkin-Elmer Spectrum one FT-IR. <sup>1</sup>H NMR and <sup>13</sup>C NMR spectra were recorded on a Bruker Avance III or JEOL spectrometer at 400 MHz and 100 MHz respectively, with TMS as an internal standard in CDCl<sub>3</sub> or DMSO-d<sub>6</sub>. <sup>31</sup>P NMR spectra were recorded on a Bruker Avance III spectrometer and were referenced to the external H<sub>3</sub>PO<sub>4</sub> at 162 MHz. Standard abbreviations indicating multiplicity were as follows: s = singlet, d = doublet, dd = doublet of doublets, t = triplet, dt = doublet of triplets, q = quadruplet and m = multiplet.

#### General procedure for the preparation of bisphosphonates

A mixture of appropriate Sulfamide **1** (1 mmol), triethyl orthoformate **2** (1.1 mmol) and diethyl phosphite **3** (3 mmol) was activated under microwave irradiation at 150 °C and 500 W for 10–20 min (reaction progress was followed by TLC monitoring every 2 minutes).

After the completion of the reaction, the reaction mixture was cooled to room temperature and purified by column chromatography using DCM/ MeOH gradient (100/0% to 96/4%).

#### Tetraethyl(((N-phenylsulfamoyl)amino)methylene)bis(phosphonate) **4a**

MF: C<sub>15</sub>H<sub>28</sub>N<sub>2</sub>O<sub>8</sub>P<sub>2</sub>S, MW: 458.40, yellow oil, R<sub>f</sub>: 0.77 (DCM/MeOH: 90/10), 162 mg, yield: 61%. IR (*ν*) 2◊NH (3413 cm<sup>−1</sup>), =C H (2928–2985 cm<sup>−1</sup>), C=C (1603 cm<sup>−1</sup>), P=O (1245 cm<sup>−1</sup>), P–O (1031 cm<sup>−1</sup>), SO<sub>2</sub> (1165 and 1393 cm<sup>−1</sup>). <sup>1</sup>H NMR (400 MHz, DMSO) δ 1.13 (t, J = 7.0 Hz, 6H, 2◊CH<sub>3</sub>), 1.19 (t, J = 7.0 Hz, 6H, 2◊CH<sub>3</sub>), 3.97–4.06 (m, 8H, 4◊CH<sub>2</sub>), 4.51 (dt, J<sub>HP</sub> = 24.0 Hz, J = 12.0 Hz, 1H, CH), 5.97 (d, J = 10.7 Hz, 1H, NH), 6.59 (t, J = 8.0 Hz, 1H<sub>Ar</sub>), 6.87 (d, J = 8.0 Hz, 2H<sub>Ar</sub>), 7.07 (t, J = 8.0 Hz, 2H<sub>Ar</sub>) ppm. <sup>13</sup>C NMR (100 MHz, DMSO) δ 16.4 (d, J<sub>CP</sub> = 6 Hz, 4◊CH<sub>3</sub>), 48.8 (t, J<sub>CP</sub> = 145.4 Hz, P–C–P), 62.3–63.5 (m, 4◊OCH<sub>2</sub>),

113.5 (<sup>3</sup>C, <sup>5</sup>C), 117.4 (<sup>4</sup>C), 129.0 (<sup>2</sup>C, <sup>6</sup>C), 147.5 (<sup>1</sup>C). <sup>31</sup>P NMR (162 MHz, DMSO):  $\delta$  18.43 ppm.

**tetraethyl (((N-(4-fluorophenyl)sulfamoyl)amino)methylene)bis(phosphonate) 4b**

MF: C<sub>15</sub>H<sub>27</sub>FN<sub>2</sub>O<sub>8</sub>P<sub>2</sub>S, MW: 476.39, yellow oil, R<sub>f</sub>: 0.78 (DCM/MeOH: 90/10), 163 mg, yield: 65%. IR ( $\nu$ ) 2 $\diamond$ NH (3289 cm<sup>-1</sup>), =C—H (2871–3074 cm<sup>-1</sup>), C=C (1597 cm<sup>-1</sup>), P=O (1236 cm<sup>-1</sup>), P—O (1012 cm<sup>-1</sup>), SO<sub>2</sub> (1150 and 1340 cm<sup>-1</sup>).

<sup>1</sup>H NMR (400 MHz, DMSO)  $\delta$  1.13 (t, J=7.0 Hz, 6H, 2 $\diamond$ CH<sub>3</sub>), 1.19 (t, J=7.0 Hz, 6H, 2 $\diamond$ CH<sub>3</sub>), 4.01–4.09 (m, 8H, 4 $\diamond$ CH<sub>2</sub>), 4.54 (dt, J<sub>HP</sub>=22.8 Hz, J=10.6 Hz, 1H, CH), 5.97 (d, J=10.7 Hz, 1H, NH), 6.92 (d, J=8.9 Hz, 2H<sub>Ar</sub>), 7.08 (d, J=8.8 Hz, 2H<sub>Ar</sub>) ppm. <sup>13</sup>C NMR (100 MHz, DMSO)  $\delta$  16.6 (d, J<sub>CP</sub>=3 Hz, 4 $\diamond$ CH<sub>3</sub>), 50.3 (t, J<sub>CP</sub>=145.4 Hz, P—C—P), 62.9 (t, J<sub>CP</sub>=3 Hz, 2 $\diamond$ OCH<sub>2</sub>), 63.1 (t, J<sub>C-P</sub>=3 Hz, 2 $\diamond$ OCH<sub>2</sub>), 115.0 (<sup>3</sup>C, <sup>5</sup>C), 120.6 (<sup>4</sup>C), 128.7 (<sup>2</sup>C, <sup>6</sup>C), 146.6 (t, J<sub>PC</sub>=5 Hz, <sup>1</sup>C). <sup>31</sup>P NMR (162 MHz, DMSO):  $\delta$  17.78 ppm.

**tetraethyl (((N-(3-fluorophenyl)sulfamoyl)amino)methylene)bis(phosphonate) 4c**

MF: C<sub>15</sub>H<sub>27</sub>FN<sub>2</sub>O<sub>8</sub>P<sub>2</sub>S, MW: 476.39, yellow oil, R<sub>f</sub>: 0.78 (DCM/MeOH: 90/10), 137 mg, yield: 55%. IR ( $\nu$ ) 2 $\diamond$ NH (3297 cm<sup>-1</sup>), =C—H (2931–3126 cm<sup>-1</sup>), C=C (1603 cm<sup>-1</sup>), P=O (1242 cm<sup>-1</sup>), P—O (1037 cm<sup>-1</sup>), SO<sub>2</sub> (1165 and 1369 cm<sup>-1</sup>). <sup>1</sup>H NMR (400 MHz, CDCl<sub>3</sub>)  $\delta$  1.24 (t, J=6.9 Hz, 6H, 2 $\diamond$ CH<sub>3</sub>), 1.29 (t, J=6.9 Hz, 6H, 2 $\diamond$ CH<sub>3</sub>), 4.07–4.29 (m, 9H, 4 $\diamond$ CH<sub>2</sub>, CH), 6.36–6.46 (m, 3H<sub>Ar</sub>), 7.09–7.11 (m, 1H<sub>Ar</sub>) ppm. <sup>13</sup>C NMR (100 MHz, CDCl<sub>3</sub>)  $\delta$  16.4 (4 $\diamond$ CH<sub>3</sub>), 50.3 (t, P—C—P, J<sub>CP</sub>=146.4 Hz), 63.7 (d, 4 $\diamond$ OCH<sub>2</sub>, J<sub>CP</sub>=36.7 Hz), 100.8 (<sup>4</sup>C), 105.3 (d, <sup>2</sup>C, J<sub>CF</sub>=36.7 Hz), 109.5 (<sup>6</sup>C), 130.5 (<sup>3</sup>C), 148.1 (<sup>1</sup>C), 162.7 (d, <sup>3</sup>C, J<sub>CF</sub>=242.4 Hz) ppm.

**tetraethyl (((N-(4-chlorophenyl)sulfamoyl)amino)methylene)bis(phosphonate) 4d**

MF: C<sub>15</sub>H<sub>27</sub>ClN<sub>2</sub>O<sub>8</sub>P<sub>2</sub>S, MW: 492.84, yellow oil, R<sub>f</sub>: 0.78 (DCM/MeOH: 90/10), 128 mg, yield: 54%. IR ( $\nu$ ) 2 $\diamond$ NH (3118 cm<sup>-1</sup>), =C—H (2984 cm<sup>-1</sup>), C=C (1599 cm<sup>-1</sup>), P=O (1244 cm<sup>-1</sup>), P—O (1025 cm<sup>-1</sup>), SO<sub>2</sub> (1159 and 1347 cm<sup>-1</sup>). <sup>1</sup>H NMR (400 MHz, DMSO)  $\delta$  1.13 (t, J=8.0 Hz, 6H, 2 $\diamond$ CH<sub>3</sub>), 1.19 (t, J=8.0 Hz, 6H, 2 $\diamond$ CH<sub>3</sub>), 3.97–4.11 (m, 8H, 4 $\diamond$ CH<sub>2</sub>), 4.53 (dt, J<sub>HP</sub>=20.0 Hz, J=8.0 Hz, 1H, CH), 6.01 (d, J=10.7 Hz, 1H, NH), 6.77 (d, J=8.0 Hz, 2H<sub>Ar</sub>), 7.34 (d, J=8.0 Hz, 2H<sub>Ar</sub>) ppm. <sup>13</sup>C NMR (100 MHz, DMSO)  $\delta$  16.1 (d, J<sub>CP</sub>=3 Hz, 4 $\diamond$ CH<sub>3</sub>), 48.0 (t, J<sub>CP</sub>=145.4 Hz, P—C—P), 62.3 (t, J<sub>CP</sub>=3 Hz, 2 $\diamond$ OCH<sub>2</sub>), 62.6 (t, J<sub>C-P</sub>=3 Hz, 2 $\diamond$ OCH<sub>2</sub>), 115.6 (C, C), 128.4 (C, C), 136.7 (C, C), 146.9 (t, J<sub>PC</sub>=3 Hz, <sup>1</sup>C) ppm.

**tetraethyl (((N-(4-iodophenyl)sulfamoyl)amino)methylene)bis(phosphonate) 4e**

MF: C<sub>15</sub>H<sub>27</sub>IN<sub>2</sub>O<sub>8</sub>P<sub>2</sub>S, MW: 584.30, brown oil, R<sub>f</sub>: 0.78 (DCM/MeOH: 90/10), 113 mg, yield: 58%. IR ( $\nu$ ) 2 $\diamond$ NH (3286 cm<sup>-1</sup>), =C—H (2916–3081 cm<sup>-1</sup>), C=C (1599 cm<sup>-1</sup>), P=O (1235 cm<sup>-1</sup>), P—O (1022 cm<sup>-1</sup>), SO<sub>2</sub> (1154 and 1343 cm<sup>-1</sup>). <sup>1</sup>H NMR (400 MHz, DMSO)  $\delta$  1.13 (t, J=7.0 Hz, 6H, 2 $\diamond$ CH<sub>3</sub>), 1.19 (t, J=7.0 Hz, 6H, 2 $\diamond$ CH<sub>3</sub>), 3.97–4.11 (m, 8H, 4 $\diamond$ CH<sub>2</sub>), 4.55 (dt, J<sub>HP</sub>=20.0 Hz, J=12.0 Hz, 1H, CH), 5.98 (d, J=10.7 Hz, 1H, NH), 6.92 (d, J=8.0 Hz, 2H<sub>Ar</sub>), 7.07 (d, J=8.0 Hz, 2H<sub>Ar</sub>) ppm. <sup>13</sup>C NMR (100 MHz, DMSO)  $\delta$  16.1 (d, J<sub>CP</sub>=3 Hz, 4 $\diamond$ CH<sub>3</sub>), 48.2 (t, J<sub>CP</sub>=145.4 Hz, P—C—P), 62.3 (t, J<sub>CP</sub>=3 Hz, 2 $\diamond$ OCH<sub>2</sub>), 62.5 (t, J<sub>C-P</sub>=3 Hz, 2 $\diamond$ OCH<sub>2</sub>), 114.4 (C, C), 120.0 (C, C), 128.1 (C, C), 146.0 (t, J<sub>PC</sub>=3 Hz, <sup>1</sup>C) ppm.

**tetraethyl (((N-(2-methoxyphenyl)sulfamoyl)amino)methylene)bis(phosphonate) 4f**

MF: C<sub>16</sub>H<sub>30</sub>N<sub>2</sub>O<sub>9</sub>P<sub>2</sub>S, MW: 488.43, yellow oil, R<sub>f</sub>: 0.78 (DCM/MeOH: 90/10), 120 mg, yield: 50%. IR ( $\nu$ ) 2 $\diamond$ NH (3116 cm<sup>-1</sup>), =C—H (2984 cm<sup>-1</sup>), C=C (1599 cm<sup>-1</sup>), P=O (1244 cm<sup>-1</sup>), P—O (1025 cm<sup>-1</sup>), SO<sub>2</sub> (1159 and 1347 cm<sup>-1</sup>). <sup>1</sup>H NMR (400 MHz, DMSO)  $\delta$  1.13 (t, J=8.0 Hz, 6H, 2 $\diamond$ CH<sub>3</sub>), 1.19 (t, J=8.0 Hz, 6H, 2 $\diamond$ CH<sub>3</sub>), 3.75 (s, 3H, OCH<sub>3</sub>), 3.99–4.13 (m, 8H, 4 $\diamond$ CH<sub>2</sub>), 4.55 (dt, J<sub>HP</sub>=20.0 Hz, J=8.0 Hz, 1H, CH), 6.01 (d, J=10.7 Hz, 1H, NH), 6.64 (t, J=8.0 Hz, 1H<sub>Ar</sub>), 7.85–7.08 (m,

3H<sub>Ar</sub>) ppm. <sup>13</sup>C NMR (100 MHz, DMSO)  $\delta$  16.1 (d, J<sub>CP</sub>=3 Hz, 4 $\diamond$ CH<sub>3</sub>), 48.0 (t, J<sub>CP</sub>=146.4 Hz, P—C—P), 55.7 (OCH<sub>3</sub>), 62.5 (t, J<sub>CP</sub>=3 Hz, 2 $\diamond$ OCH<sub>2</sub>), 62.8 (t, J<sub>C-P</sub>=3 Hz, 2 $\diamond$ OCH<sub>2</sub>), 113.4 (C), 122.5 (C, C), 128.8 (<sup>3</sup>C), 129.1 (<sup>1</sup>C), 147.9 (t, J<sub>PC</sub>=3 Hz, <sup>2</sup>C) ppm.

**In vitro anti-inflammatory activity**

*In vitro* anti-inflammatory activity was evaluated by the method of Karthik *et al.*<sup>[65]</sup> with slight changes. Briefly, 100  $\mu$ L of 0.033 mM dose of **4a**, **4b**, **4c** and **4d** or 0.026 mM of diclofenac were added to 1 mL of solution of 0.2 % ovalbumin prepared in Tris-HCl (pH : 6.6), the solutions are kept for 15 min at (37 °C) in the incubator. After that, they are maintained in a water bath for five minutes at (72 °C). Then the cooling turbidity was determined at 660 nm using UV-visible spectrophotometer. For each molecule of sulfamide-

containing bisphosphonate, a white was prepared in 1 ml extract and 1 ml Tris-HCl.

The percentage inhibition of protein denaturation represents the percentage of anti-inflammatory activity, which was calculated using the following formula:

$$\% \text{ inhibition of denaturation} = \frac{\text{absorption of the diclofenac} - \frac{1}{4} \text{ absorption of the test sample}}{\text{absorption of the diclofenac}} \times 100$$

**Computational details**

Computational techniques such as the density functional theory (DFT), ADMET evaluation, and molecular docking were performed to the previously synthesized molecules **4a**, **4b**, **4c** and **4d** for explaining the reactivity and selectivity of various types of organic reaction,<sup>[66]</sup> and to elucidate the chemical nature, drug likeness and

anti-inflammatory activity of molecules,<sup>[67]</sup> also predicts drug-receptor interactions that hold a protein and a ligand together in a bound state.<sup>[68]</sup>

**Ligand preparation**

The 3D chemical structures of the synthesized molecules were transferred as MDL Mol file from Chemdraw 3D software (Chem-Draw, 2019) to gaussian 09 software (Gaussian 09). First, the structures were pre-optimized with semi-empirical AM1 method

using gaussian 09 software.<sup>[69]</sup> Then they were optimized using Gaussian 09 software. <sup>13</sup>C NMR (100 MHz, DMSO)  $\delta$  114.4 (C, C), 120.0 (C, C), 128.1 (C, C), 146.0 (t, J<sub>PC</sub>=3 Hz, <sup>1</sup>C) ppm.

density functional theory DFT method by employing the B3LYP/6-31G (d,p) basis set to obtain the most stable conformation,<sup>[10-11]</sup> which was also used to calculate the global reactivity descriptors. Molecular electrostatic potential (MEP) maps of the optimized structure were calculated and generated with Gauss view 5

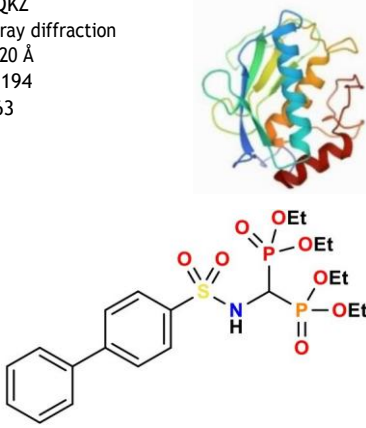
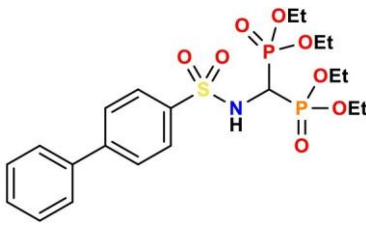
software. The optimized structures were combined in one database on MOE 2015 software (Molecular Operating Environment) in order to study the affinity of the ligands.

### Protein preparation

The crystal structure of Matrix Metalloproteinase (MMP-8) at a resolution of 1.20 Å, was retrieved from Protein databank (<http://www.rcsb.org>) with their PDB identification code (PDB ID: 4QKZ).<sup>[72]</sup> (Table 6) A resolution between 1.5 and 2.5 Å is considered as a good quality for docking studies.<sup>[73]</sup> The sequence of the protein was edited by removing co-factors using default parameters included in MOE software. The water molecules were inserted in the active site of the target enzyme for their important role to ensure making hydrogen bonds between the ligand and the target.<sup>[74]</sup> After that, the protein structure was prepared by correcting the missing bonds, which were broken in X-Ray diffraction, and then the hydrogen atoms were added. The active site was searched using the site finder tool.

### Molecular docking

Virtual screening calculations were carried out using standard default parameters settings in the MOE Software package (molecular operating environment MOE, 2015). First, the co-crystallized ligand is docked into the binding site pocket of MMP-8. Then the compounds-ligands **4(a–d)** were oriented in flexible conformation for docking when protein was kept in a rigid conformation. The best conformations of the ligand were analyzed for their binding interactions and were evaluated by binding free energies (S-score, Kcal/mol), and bonds interactions between ligand atoms and active site residues. It is known that the best energy score should be less or equal to  $-7$  Kcal/mol.<sup>[75]</sup> Thus, targets showing the higher binding energy of docking score were considered as the worst molecules in inhibiting the target receptor, as the higher binding energy corresponds to lower binding affinity.<sup>[75]</sup> This value is often used as criterion to validate the results of the molecular docking.

Table 6. Details related to Matrix Metalloproteinase (MMP-8).		
	MMP-8	3D Structure of MMP-8
Code	4QKZ	
Method	X-ray diffraction	
Resolution	1.20 Å	
R-value	0.194	
Residues number	163	
Co-crystallized ligand		

### Global reactivity descriptors

Nowadays, calculation-based methods have become very popular for studying the Structure-Activity Relationships (SAR) of compounds. Density Functional Theory (DFT) is one of the most widely used chemical property calculation methods in theoretical chemistry, as it allows dealing with the correlation of systems comprising a large number of electrons, almost at the cost of a Hartree-Fock calculation.<sup>[76]</sup>

Herein, a theoretical research has investigated by employing density functional theory (DFT) at the **B3LYP** level with the 6-31G (d,p) basis set. Further, various parameters, geometry optimization and reactivity indices analysis are computationally calculated.

### Ligand based druglikeness, ADME/toxicity

Many potential therapeutic agents fail to reach the clinical trials for their unfavorable ADME parameters. To estimate likelihood of our synthesized products to pass the clinic trials, we calculate *in-silico* the Lipinski's rule of five,<sup>[77]</sup> Veber's rule,<sup>[78]</sup> Egan's rule,<sup>[79]</sup> and Polar surface area (TPSA), number of rotatable, the ADME/Toxicity (pharmacological and pharmacodynamic) properties using SwissADME properties calculation online, PASS-Way2Drug server, PKCSM server and Swiss target prediction.

### Supporting Information Summary

The IR and <sup>1</sup>H, <sup>13</sup>C, <sup>31</sup>P NMR spectra of the synthesized compounds are available in the supporting information.

### Acknowledgements

This work was supported financially by The General Directorate for Scientific Research and Technological Development (DG-RSDT), Algerian Ministry of Scientific Research, Applied Organic Laboratory (FNR 2000). This research has been carried out within the PRFU project (2021; ref B00L01UN230120200006).

### Conflict of Interest

The authors declare no conflict of interest.

### Data Availability Statement

The data that support the findings of this study are available from the corresponding author upon reasonable request.

**Keywords:** Anti-inflammatory Activity • Bisphosphonate • DFT study • Microwave-assisted synthesis • Molecular Docking

- [1] G. A. Petroianu, *Pharmazie*. **2011**, *66*, 804-807.
- [2] N. B. Watts, C. H. Chesnut, H. K. Genant, S. T. Harris, R. D. Jackson, A. A. Licata, P. D. Miller, W. J. Mysiw, B. Richmond, D. Valent, *Bone*. **2020**, *134*, 115222.
- [3] A. Ioachimescu, A. Licata, *Curr. Osteoporos. Rep.* **2007**, *5*, 165-169.
- [4] R. G. G. Russell, *Pediatrics*. **2007**, *119*, S150-S162.
- [5] B. Aderibigbe, I. Aderibigbe, P. Popoola, *Pharmaceutica* **2017**, *9*, 2.
- [6] D. L. Diab, N. B. Watts, P. D. Miller, *Osteoporos.* **2013**, 1859-1872.
- [7] Y. Saunders, J. R. Ross, K. E. Broadley, P. M. Edmonds, S. Patel, *Palliat Med.* **2004**, *18*, 418-431.

- [8] H. S. Yeh, J. R. Berenson, *Clin. Cancer Res.* **2006**, *12*, 6279s-6284 s.
- [9] F. Wolfe, M. B. Bolster, C. M. O'Connor, K. Michaud, K. W. Lyles, C. S. Colón-Emeric, *J. Bone Miner. Res.* **2013**, *28*, 984-991.
- [10] I. Holen, E. R. Coleman, *Curr. Pharm. Des.* **2010**, *16*, 1262-1271.
- [11] R. A. Nadar, N. Margiotta, M. Iafisco, J. J. P. van den Beucken, O. C. Boerman, S. C. G. Leeuwenburgh, *Adv. Healthcare Mater.* **2017**, *6*, 1601119.
- [12] W. P. Maksymowych, *Curr. Med. Chem.* **2002**, *1*, 15-28.
- [13] C. Korkmaz, S. Demirbaş, D. M. Yavşan, P. Oltulu, I. Kılıç, M. Uyar, *Med J.* **2019**, *59*, 110-115.
- [14] A. Kane, L. Campbell, D. Ky, D. Hibbs, D. Carter, *Antimicrob. Agents Chemother.* **2020**, *65*, e01753-20.
- [15] M. A. Ermer, S. C. Kottmann, J.-E. Otten, A. Wittmer, P. Poxleitner, K. Pelz, *JOMS.* **2018**, *76*, 553-560.
- [16] E. Chmielewska, P. Kafarski, *Open Pharm Sci J.* **2016**, *3*, 56-78.
- [17] N. Pavlakis, M. Stockler, *Cochrane Database Syst. Rev.* **1996**, *20*, CD003474.
- [18] J. C. B. Santos, J. A. de Melo, S. Maheshwari, W. M. T. Q. de Medeiros, J. W. de Freitas Oliveira, C. J. Moreno, L. Amzel, S. B. Gabelli, M. Sousa Silva, *Molecules.* **2020**, *25*, 2602-2621.
- [19] P. Kafarski, B. Lejczak, G. Forlani, *Heteroat. Chem.* **2000**, *11*, 449-453.
- [20] A. Saad, W. Zhu, G. Rousseau, P. Mialane, J. Marrot, M. Haouas, F. Taulelle, R. Dessapt, H. Serier-Brault, E. Rivière, T. Kubo, E. Oldfield, A. Dolbecq, *Chem. Eur. J.* **2015**, *21*, 10537-10547.
- [21] E. Gumienna-Kontecka, J. Jezierska, M. Lecouvey, Y. Leroux, H. Kozłowski, *J. Inorg. Biochem.* **2002**, *89*, 13-17.
- [22] F. C. Teixeira, C. Lucas, M. J. M. Curto, A. P. S. Teixeira, M. T. Duarte, V. André, *Heteroat. Chem.* **2015**, *27*, 3-11.
- [23] A. Laghezza, L. Piemontese, L. Brunetti, A. Caradonna, M. Agamennone, F. Loiodice, P. Tortorella, *Pharmaceuticals (Basel).* **2021**, *14*, 85-99.
- [24] R. Lenin, R. M. Raju, D. V. N. S. Rao, U. K. Ray, *Med. Chem. Res.* **2012**, *22*, 1624-1629.
- [25] M. T. Rubino, M. Agamennone, C. Campestre, P. Campiglia, V. Cremasco, R. Faccio, A. Laghezza, F. Loiodice, D. Maggi, E. Panza, A. Rossello, P. Tortorella, *ChemMedChem.* **2011**, *6*, 1258-1268.
- [26] M. Sudileti, S. Nagaripati, M. Gundluru, V. Chintha, S. Aita, R. Wudayagiri, N. Chamarthi, S. R. Cirandur, *ChemistrySelect.* **2019**, *4*, 13006-13011.
- [27] H. Xiang, X. Qi, Y. Xie, G. Xu, C. Yang, *Org. Biomol. Chem.* **2012**, *10*, 7730-7738.
- [28] B. Akgun, D. Avci, *J. Polym. Sci. A: Polym. Chem.* **2012**, *50*, 4854-4863.
- [29] S. Siva Prasad, S. H. Jayaprakash, C. Syamasundar, P. Sreelakshmi, C. Bhuvaneshwar, B. Vijaya Bhaskar, W. Rajendra, S. K. Nayak, C. Suresh Reddy, *Phosphorus Sulfur Silicon Relat. Elem.* **2015**, *190*, 2040-2050.
- [30] X. Yang, S. Akhtar, S. Rubino, K. Leifer, J. Hilborn, D. Ossipov, *Chem. Mater.* **2012**, *24*, 1690-1697.
- [31] D. Thakre, S. R. Ali, S. Mehta, N. Alam, M. Ibrahim, D. Sarma, A. Mondal, M. De, A. Banerjee, *Cryst. Growth Des.* **2021**, *21*, 4285-4298.
- [32] E. Chmielewska, P. Kafarski, *Molecules.* **2016**, *21*, 1474-1500.
- [33] S. Poola, M. Gundluru, M. R. Nadevedhi, M. S. P. T. S. R. K. P. R. Saddala, S. R. Cirandur, *Phosphorus Sulfur Silicon Relat. Elem.* **2019**, *195*, 409-420.
- [34] R. Aufaure, Y. Lalatonne, N. Lièvre, O. Heintz, L. Motte, E. Guénin, *RSC Adv.* **2014**, *4*, 59315-59322.
- [35] S. S. Reddy, R. M. N. Kalla, A. Varyambath, I. Kim, *Catal. Commun.* **2019**, *126*, 15-20.
- [36] U. M. R. Kunda, S. K. Balam, B. R. Nemallapudi, S. S. Cherreddy, S. K. Nayak, S. R. Cirandur, *Chem. Pharm. Bull.* **2012**, *60*, 104-109.
- [37] S. Tellamekala, M. Gundluru, M. Sudileti, S. Sarva, C. Rohini, K. Putta, S. Reddy Cirandur, *Monatsh. Chem.* **2020**, *151*, 251-260.
- [38] B. Kaboudin, S. A. Alipour, *Tetrahedron Lett.* **2009**, *50*, 4243-4245.
- [39] E. Bálint, A. Tajti, A. Dzielak, G. Hägele, G. Keglevich, *Beilstein J. Org. Chem.* **2016**, *12*, 1493-1502.
- [40] A. Amira, H. K'tir, I. Becheker, S. Ouarna, N. Inguibert, H. Berredjem, M. Berredjem, N.-E. Aouf, *Der Pharma Chem.* **2015**, *7*, 213-219.
- [41] H. K'tir, Z. Aouf, T. O. Souk, R. Zerrouki, M. Berredjem, N.-E. Aouf, *Phosphorus Sulfur Silicon Relat. Elem.* **2016**, *192*, 555-559.
- [42] Z. Aouf, S. Bouacida, C. Benzaid, A. Amira, H. K'tir, M. Mathé-allainmat, J. Lebreton, N.-E. Aouf, *ChemistrySelect.* **2021**, *6*, 9722-9727.
- [43] H. K'tir, A. Amira, C. Benzaid, Z. Aouf, S. Benharoun, Y. Chemam, R. Zerrouki, N.-E. Aouf, *J. Mol. Struct.* **2022**, *1250*, 131635.
- [44] J. J. Jun, X. Xie, *ChemistrySelect* **2021**, *6*, 430-469.
- [45] E. Berrino, S. Bua, M. Mori, M. Botta, V. S. Murthy, V. Vijayakumar, Y. Tamboli, G. Bartolucci, A. Mugelli, E. Cerbai, C. T. Supuran, F. Carta, *Molecules.* **2017**, *22*, 1049-1066.
- [46] J.-Y. Winum, A. Scozzafava, J.-L. Montero, C. T. Supuran, *Med. Res. Rev.* **2006**, *26*, 767-792.
- [47] A. B. Reitz, G. R. Smith, M. H. Parker, *Expert Opin. Ther. Pat.* **2009**, *19*, 1449-1453.
- [48] L. Gavernet, I. A. Barrios, M. S. Cravero, L. E. Bruno-Blanch, *Bioorg. Med. Chem.* **2007**, *15*, 5604-5614.
- [49] A. Jabłońska-Trypuć, M. Matejczyk, S. Rosochacki, *J. Enzyme Inhib. Med. Chem.* **2016**, *31*, 177-183.
- [50] K. Li, F. R. Tay, C. K. Y. Yiu, *Pharmacol. Ther.* **2020**, *207*, 107465.
- [51] A. Alaseem, K. Alhazzani, P. Dondapati, S. Alobid, A. Bishayee, A. Rathinavelu, *Semin. Cancer Biol.* **2019**, *56*, 100-115.
- [52] E.-S. E. Mehana, A. F. Khafaga, S. S. El-Blehi, *Life Sci.* **2019**, *234*, 116786.
- [53] O. Teronen, P. Heikkilä, Y. T. Konttinen, M. Laitinen, T. Salo, R. Hanemaaijer, A. Teronen, P. Maisi, T. Sorsa, *Ann. N. Y. Acad. Sci.* **1999**, *878*, 453-465.
- [54] M. Tauro, A. Laghezza, F. Loiodice, M. Agamennone, C. Campestre, P. Tortorella, *Bioorg. Med. Chem.* **2013**, *21*, 6456-6465.
- [55] H. Valleala, R. Hanemaaijer, J. Mandelin, A. Salminen, O. Teronen, J. Mönkkönen, Y. T. Konttinen, *Life Sci.* **2003**, *73*, 2413-2420.
- [56] W. Boufas, N. Dupont, M. Berredjem, K. Berrezag, I. Becheker, H. Berredjem, N.-E. Aouf, *J. Mol. Struct.* **2014**, *1074*, 180-185.
- [57] C. Mouffouk, L. Hambaba, H. Haba, S. Mouffouk, C. Bensouici, S. mouffouk, M. Hachemi, H. Khadraoui, *Orient. Pharm. Exp. Med.* **2018**, *18*, 335-348.
- [58] N. H. Grant, H. E. Alburn, C. Kryzanasukas, *Biochem. Pharmacol.* **1970**, *19*, 715-722.
- [59] a) K. N. Houk, *J. Am. Chem. Soc.* **1973**, *95*, 4092-4094; b) K. N. Houk, *Acc. Chem. Res.* **1975**, *8*, 361-369.
- [60] R. G. Parr, W. Yang, *Annu. Rev. Phys. Chem.* **1995**, *46*, 701-728.
- [61] P. Geerlings, F. D. Proft, W. Langenaeker, *Chem. Rev.* **2003**, *103*, 1793-1874.
- [62] L. R. Domingo, M. Ríos-Gutiérrez, P. Pérez, *Molecules* **2016**, *21*, 748-769.
- [63] R. Thomsen, M. H. Christensen, *J. Med. Chem.* **2006**, *49*, 3315-3321.
- [64] J. A. Jacobsen, J. L. Major Jourden, M. T. Miller, S. M. Cohen, *Biochim. Biophys. Acta Mol. Cell Res.* **2010**, *1803*, 72-94.
- [65] K. Karthik, P. B. R. Kumar, R. V. Priya, K. S. Kumar, R. S. B. Rathore, *IJRPB.* **2013**, *1*, 729-731.
- [66] W. Yahia, A. N. Khorief, M. Liacha, *Prog. React. Kinet.* **2014**, *39*, 365-374.
- [67] N. T. El-Shamy, A. M. Alkaoud, R. K. Hussein, M. A. Ibrahim, A. G. Alhamzani, M. M. Abou-Krishna, *Molecules.* **2022**, *27*, 1-17.
- [68] O. Silakari, K.-S. Pankaj, Chapter 6 - Molecular docking analysis: Basic technique to predict drug-receptor interactions: *Concepts and Experimental Protocols of Modelling and Informatics in Drug Design*, **2021**, 131-155.
- [69] J. J. P. Stewart, *J. Mol. Model.* **2013**, *19*, 1-32.
- [70] A. D. Becke, *J. Chem. Phys.* **1997**, *107*, 8554-8560.
- [71] M. J. Frisch, G. W. Trucks, H. B. Schlegel, G. E. Scuseria, M. A. Robb, J. R. Cheeseman, G. Scalmani, V. Barone, B. Mennucci, G. A. Petersson, H. Nakatsuji, M. Caricato, X. Li, H. P. Hratchian, A. F. Izmaylov, J. Bloino, G. Zheng, J. L. Sonnenberg, M. Hada, M. Ehara, K. Toyota, R. Fukuda, J. Hasegawa, M. Ishida, T. Nakajima, Y. Honda, O. Kitao, H. Nakai, T. Vreven, J. A. Montgomery Jr., J. E. Peralta, F. Ogliaro, M. Bearpark, J. J. Heyd, E. Brothers, K. N. Kudin, V. N. Staroverov, R. Kobayashi, J. Normand, K. Raghavachari, A. Rendell, J. C. Burant, S. S. Iyengar, J. Tomasi, M. Cossi, N. Rega, J. M. Millam, M. Klene, J. E. Knox, J. B. Cross, V. Bakken, C. Adamo, J. Jaramillo, R. Gomperts, R. E. Stratmann, O. Yazyev, A. J. Austin, R. Cammi, C. Pomelli, J. W. Ochterski, R. L. Martin, K. Morokuma, V. G. Zakrzewski, G. A. Voth, P. Salvador, J. J. Dannenberg, S. Dapprich, A. D. Daniels, Ö. Farkas, J. B. Foresman, J. V. Ortiz, J. Cioslowski, and D. J. Fox, Gaussian 09, Revision D.01. Gaussian, Inc., Wallingford CT, **2009**.
- [72] G. Pochetti, R. Montanari, D. Capelli, P. Tortorella, X-ray structure of the catalytic domain of MMP-8 with the inhibitor ML115, [https://ftp.wwpdb.org/pub/pdb/validation-reports/qk/4qkz/4qkz\\_full-validation.pdf.gz](https://ftp.wwpdb.org/pub/pdb/validation-reports/qk/4qkz/4qkz_full-validation.pdf.gz).
- [73] C. Venugopal, C. M. Demos, K. S. Jagannatha Rao, M. A. Pappolla, K. Sambamurti, *CNS Neurol. Disord. Drug Targets* **2008**, *7*, 278-294.
- [74] a) H. J. Böhm, G. Schneider, R. Mannhold, H. Kubinyi, G. Folkers, Protein-ligand interactions: From molecular Recognition to Drug Design, WILEY-

VCH Verlag GmbH & Co. KGaA, Weinheim, **2005** ; b) G. Klebe, *Drug Discovery Today* **2006**, *11*, 580-94 ; c) Y. Marechal, *The Hydrogen Bond and the Water Molecule : the physics and chemistry of water, aqueous and bio media*, Elsevier, **2007**.

[75] L. Simon, A. Lmane, K. K. Srinivasan, L. Pathak, I. Daoud, *Interdiscip. Sci.* **2017**, *9*, 445-458.

[76] A. Ponti, *Molecules*. **2020**, *25*, 5301.

[77] C. A. Lipinski, F. Lombardo, B. W. Dominy, P. J. Feeney, *Adv. Drug Delivery Rev.* **2001**, *46*, 3-26.

[78] D. F. Veber, S. R. Johnson, H. Y. Cheng, B. R. Smith, K. W. Ward, K. D. Kopple, *J. Med. Chem.* **2002**, *45*, 2615-23.

[79] W. J. Egan, K. M. Merz, J. J. Baldwin, *J. Med. Chem.* **2000**, *43*, 3867-3877.

Submitted: May 14, 2022

Accepted: July 13, 2022